8. Progressive Collapse Analysis of a Ship's Hull under Longitudinal Bending

by Tetsuya Yao*, *Member* Plamen Ivanov Nikolov**, *Member*

Summary

From the viewpoints of safety and economy, it is very important to estimate the load carrying capacity of a ship's hull as a whole. For this purpose, a simple method was proposed to simulate progressive collapse behaviour of a ship's hull subjected to longitudinal bending. In this method, the cross-section of a hull girder is divided into small elements consisting of a stiffener and attached plating. For each stiffener element, the average stress-strain relationship under axial load is derived based on the equilibrium conditions of forces and moments. The buckling and yielding both in stiffeners and plates are taken into account. Then, curvature is incrementally applied to the hull girder cross-section assuming that plane-sections remain plane. At each incremental step, the tangential flexural rigidity of a cross-section is evaluated using the tangential slope of the average stress-strain curves of individual elements, and hence the increment of bending moment is evaluated.

Performing example calculations on existing test girder models under bending, the rationality of the proposed method was examined. Then, the analysis was performed on an existing bulk carrier, and the progressive collapse bahaviour of the cross-section under longitudinal bending was discussed. It was found that the fully plastic bending moment can not be sustained at the cross-section due to buckling of compressed members in the cross-section. It was also found that the maximum bending moment carried at the cross-section under the sagging condition is 20% lower than that under the hogging condition.

1. Introduction

A ship's hull is a typical box girder structure, and is subjected to longitudinal bending due to distributed weights, buoyancy forces and wave loads. To design a ship's hull that withstands these loads, some allowable stresses have been introduced in a structural design so that the deck and/or bottom plating do not undergo buckling/plastic collapse. From this point of view, many research works have been performed on buckling/plastic collapse strength of isolated plates and stiffened plates both theoretically and experimentally, and useful results have been obtained.

At the same time, it is very important to know the load carrying capacity of a ship's hull as a whole from the viewpoints of safety and economy. Such informations may fundamentally be obtained by performing FEM analysis on a ship's hull that considers both material and geometrical nonlinearities.[1,2] However, such analysis may require excessive efforts and computing time even with today's super computers. For that, some simplified method is required. As far as the maximum bending moment carried at a girder cross-section is concerned, simple methods were proposed by Nishihara[3] and Endo et. al.[4] In their methods, however, the reduction in load carrying capacity of individual members after their ultimate strength is not considered, although the ultimate bending moment was estimated with fairly good accuracy.

On the other hand, Ueda et.al.[5] developed efficient elements for plates and stiffened plates under biaxial tensile and/or compressive and shear loads. In their method, a stiffened panel surrounded by longitudinal and transverse girders is considered as one element, and the stiffness matrix is derived for this large unit considering the influences of buckling and yielding. This work was done in the framework of the Idealized Structural Unit Method (ISUM).[6] Applying the improved unit, Paik[7,8] simulated the collapse behaviour of ship's hull girders subjected to longitudinal bending moment.

Smith et.al.[9-13] proposed another simple but efficient method to analyse progressive collapse behaviour of box girder structures under longitudinal bending. The fundamental idea of Smith's method is based on that by Caldwell,[14] but his method takes into account of the progressive loss in stiffness of a cross-section due to buckling and yielding in structural components. Smith described the procedure of his method as follows:[9]

* Faculty of Engineering, Hiroshima University
** Graduate School of Engineering, Hiroshima University

"(i) the hull cross-section is divided into small elements;
(ii) vertical curvature of the hull is assumed to occur incrementally; correpsponding incremental element strains are calculated on the assumption that plane-sections remain plane and that bending occurs about the instantaneous elastic neutral axis of the cross-section;
(iii) element incremental stresses are derived from incremental strains using the slopes of stress-strain curves;
(iv) element stresses are integrated over the cross-section to obtain bending moment increments; incremental curvatures and bending moments are summed to provide cumulative values."

His method may be regarded as a rather simple method comparing to ISUM, but easily gives solutions which is accurate enough under pure bending. The only difficulty in Smith's method is the derivation of average stress-strain relationships of component elements taking into account of buckling and yielding. To obtain such stress-strain relationships, Smith performed elastoplastic large deflection FEM analysis. Such analysis may require much works especially when the number of elements becomes large.

In the present paper, the average stress-strain relationships of elements were derived in an analytical manner. Then, according to the Smith's method, a computer code "HULLST" was developed to analyse the progressive collapse behaviour of the cross-section of a hull girder subjected to longitudinal bending. After performing example calculations on existing girder specimens to check the rationality of the proposed method, progressive collapse behaviour of the cross-section of an existing bulk carrier of 60,000 DWT was analysed both under sagging and hogging conditions.

2. Method of Analysis

2.1 General Assumptions

The longitudinal stiffening system is usually employed in large ships at their midlength part, and the deck, bottom and side plating are stiffened by a number of longitudinal stiffeners and girders. If an extreme bending load acts on a hull girder, the most possible collapse mode may be the overall collapse of stiffened panel after local collapse of individual plates between stiffeners. In the following, such collapse mode is assumed to derive average stress-strain relationships of elements.

Figure 1 shows a typical element consisting of a stiffener and attached plating. When this element is subjected to compressive load in the axial direction, the stiffener may deflect as indicated in Fig. 1 (b). In this case, three types of modeling may be possible, which are two single span models, AB and BC, and a double span model, *12*. Among them, the double span model may be most rational and only this model is considered.

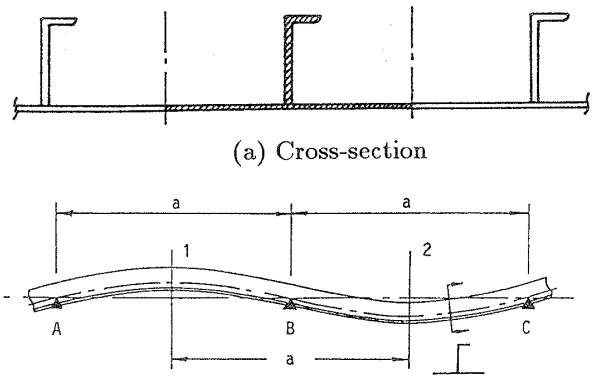

(a) Cross-section

(b) Deflection mode under axial compression

Fig. 1 Element for progressive collapse analysis

To derive average stress-strain relationship of a stiffener element, the following assumptions are made:
(1) Attached platings behave as isolated plates.
(2) Plane cross-sections remain plane, and the strain varies linearly over the cross-section.
(3) The material is assumed to be elastic-perfectly plastic.
(4) The deformation in torsional buckling mode of a stiffener is not considered.

The average stress-strain relationships of isolated plates are derived combining the results of elastic large deflection analysis and rigid plastic mechanism analysis. Those of stiffener elements are derived considering elastoplastic stress distributions at both ends of the element which satisfy the equilibrium conditions of forces and moments.

2.2 Average stress-strain relationships of isolated plates

2.2.1 Initial imperfections due to welding and deflection mode under thrust

When longitudinal stiffening system is employed, the dominant compressive and/or tensile load acts on the plate in the direction of its longer side as indicated in Fig. 2. All sides are assumed to be simply supported and remain straight while subjected to in-plane movements.

The plates in a ship structure usually contain welding residual stresses and initial deflection associated by fillet welding of stiffeners to the plating. In this paper, a rectangular distribution of welding residual stresses is assumed considering the continuity condi-

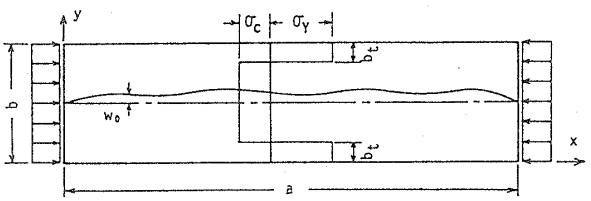

Fig. 2 Rectangular plate with initial imperfections due to welding

tion of plates. From the self equilibrium condition of residual stresses, the following relationship is derived.

$$2b_t\sigma_Y = (b-2b_t)\sigma_c \tag{1}$$

The general form of initial deflection may be expressed as:

$$w_0 = \sum_{m=1}^{\infty} A_{0m} \sin\frac{m\pi x}{a} \sin\frac{\pi y}{b} \tag{2}$$

and the total deflection under inplane compressive load as:

$$w = \sum_{m=1}^{\infty} A_m \sin\frac{m\pi x}{a} \sin\frac{\pi y}{b} \tag{3}$$

However, it is known that only a single deflection term is amplified while other components become negligibly small with the increase of compressive load above buckling load until secondary buckling takes place.[15] Consequently, the behaviour of a plate can be approximated by taking single deflection modes, A_{0m} and A_m in Eqs.(2) and (3), respectively. m is a number of half-waves of a stable deflection mode above buckling load, and is taken as:

$m = 1$ for $a/b \leq 1.3$
$m = n$ for $n - 0.7 < a/b \leq n + 0.3$

where a/b is the aspect ratio of the plate, and n is an integer greater than 1. Hereafter, A_{0m} and A_m are denoted as A_0 and A, respectively.

2.2.2 Relationship between average stress and deflection

Performing elastic large deflection analysis, the relationship between average compressive stress, σ, and deflection, A, is derived as follows.[16]

$$\frac{E\pi^2}{16b^2}(1/\alpha^2+\alpha^2)(A^2-A_0^2)$$

$$+\sigma_{cr0}(1-A_0/A)-\sigma$$

$$-\frac{\sigma_Y}{\pi}\frac{\sin\mu\pi}{(1-\mu)} = 0 \tag{4}$$

where $\alpha = a/mb$ and

$$\sigma_{cr0} = \frac{Et^2\pi^2}{12(1-\nu^2)b^2}(1/\alpha+\alpha)^2 \tag{5}$$

$$\mu = \sigma_c/(\sigma_Y+\sigma_c) = 2b_t/b \tag{6}$$

The relationship between average stress and deflection is derived also according to the plastic mechanism analysis assuming rigid-perfectly plastic material. Depending on the aspect ratio, a/b, of the plate, two sets of plastic mechanism may exist as illustratred in Fig.3. For each mechanism, the following relationships are derived.[17]

$\alpha \leq 1.0$

$$m_{45} + (1/\alpha - 1)m_{90}/2 = (2/\alpha - 1)\overline{\sigma}\overline{A} \tag{7}$$

$\alpha > 1.0$

$$m_{45} + (\alpha - 1)m_0/2 = \overline{\sigma}\overline{A} \tag{8}$$

where $\overline{\sigma} = \sigma/\sigma_Y$, $\overline{A} = A/t$ and

$$m_{90} = 1 - \overline{\sigma}^2 \tag{9}$$

$$m_0 = 2m_{90}/\sqrt{1+3m_{90}} \tag{10}$$

$$m_{45} = 4m_{90}/\sqrt{1+15m_{90}} \tag{11}$$

The average stress-deflection relationship changes from that expressed by Eq.(4) to that by Eq.(7) or Eq.(8) at their intersection, which gives the compressive ultimate strength.

2.2.3 Relationship between average stress and average strain

According to the elastic large deflection analysis, the average strain is expressed in terms of the average stress and deflection as follows.[16]

$$\varepsilon = \sigma/E + (m^2\pi^2/8a^2)(A^2-A_0^2) \tag{12}$$

On the other hand, the average strain by plastic mechanism analysis is expressed as:

$\alpha \leq 1.0$

$$\varepsilon = \sigma/E + (2m^2/a^2)(A^2-A_0^2) \tag{13}$$

$\alpha > 1.0$

$$\varepsilon = \sigma/E + (2m^2/ab)(A^2-A_0^2) \tag{14}$$

Until the compressive ultimate strength is attained, the average stress-strain relationship is expressed by Eq.(12). At the ultimate strength, the strain is assumed to increase from the value evaluated by Eq.(12) to that by Eq.(13) or Eq.(14). After this, the average

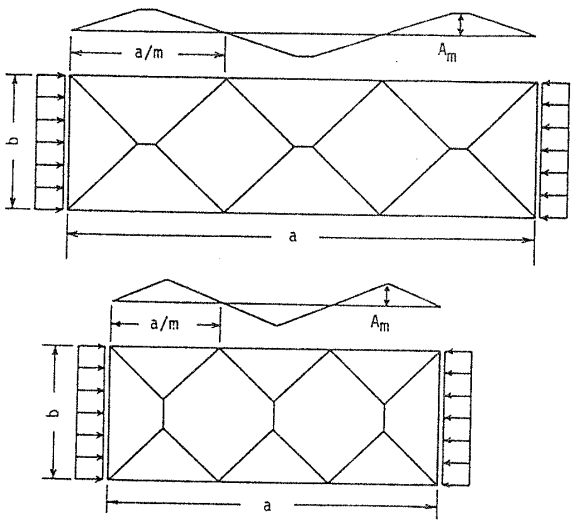

Fig. 3 Plastic mechanism of plate under thrust

stress-strain relationship is expressed by Eq.(13) or Eq.(14).

Here, when a plate is thick and undergoes plastic buckling, the inplane plastic strain until buckling is not considered, since the first term in Eqs.(12), (13) and (14) represents the elastic inplane strain, and the second term the strain produced by lateral deflection. For such a case, a constant value evaluated as the difference between the buckling strain calculated elastically and the yield strain is added to the strain after the ultimate strength has been attained.

When a stiffener element is subjected to tensile axial force, the stress-strain relationship of an elastic-perfectly plastic material is assumed as the average stress-strain relationship in a tensile range.

2.2.4 Influence of welding residual stresses

When there exist welding residual stresses as illustrated in Fig.2, the compressive load is not carried at the central part of the plate after this part has been yielded under compressive load but is carried only at the side parts where residual stresses are in tension. For this stage, the tangential inplane rigidity can be approximated by $2b_tE/b$. That is, when the ultimate strength is greater than $\sigma_Y - \sigma_c$, the tangential inplane rigidity is set equal to $2b_tE/b$ at the stress level higher than $\sigma_Y - \sigma_c$.

On the other hand, when tensile load is applied, the side parts can not carry tensile load, since these parts are already yielded in tension. In this case, the tangential rigidity is expressed as:

$$d\sigma/d\varepsilon = (1 - 2b_t/b)E \qquad (15)$$

The influences of welding residual stresses on plate behaviour both under tensile and compressive loading are schematically shown in Fig. 4. The decrease in buckling strength due to welding residual stresses is automatically evaluated when Eq.(4) is used.

2.2.5 Accuracy of stress-strain relationship by the proposed method

To examine the accuracy of the average stress-strain relationship of a plate derived by the proposed method, a series of elastoplastic large deflection FEM analysis was performed. Calculated stress-deflection curves for the plate of $a/b = 0.8$ are plotted in Fig.5 (a) together with those by Eq.(7). It is seen that the deflection produced by the plastic mechanism analysis is smaller than that by FEM analysis. This may be partly because the elastic deflection component is ignored in Eq.(7). Although more precise discussion is necessary on this, the deflection is modyfied by deviding $\overline{\sigma}$ to get better agreement with that by FEM analysis. That is, Eqs.(7) and (8) are modified as follows:

$\alpha \leq 1.0$

$$m_{45} + (1/\alpha - 1)m_{90}/2 = (2/\alpha - 1)\overline{\sigma}^2\overline{A} \qquad (16)$$

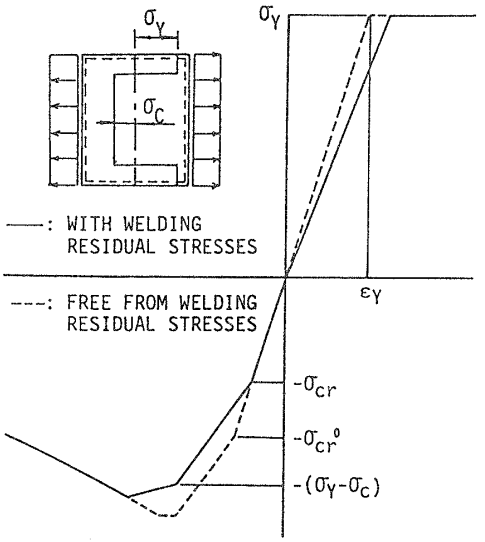

Fig. 4 Influence of welding residual stresses on plate behaviour under inplane load

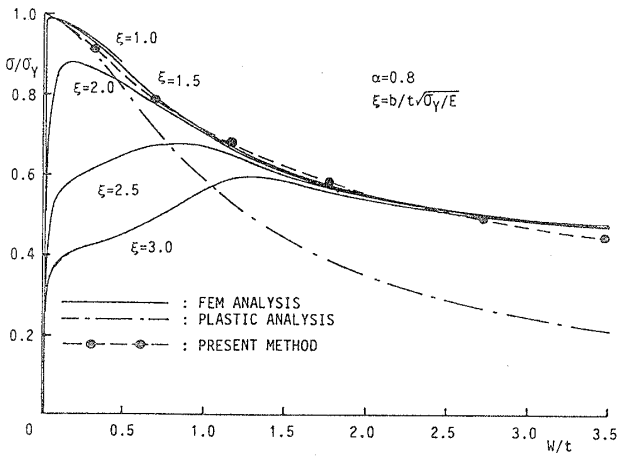

(a) Average stress-deflection relationships

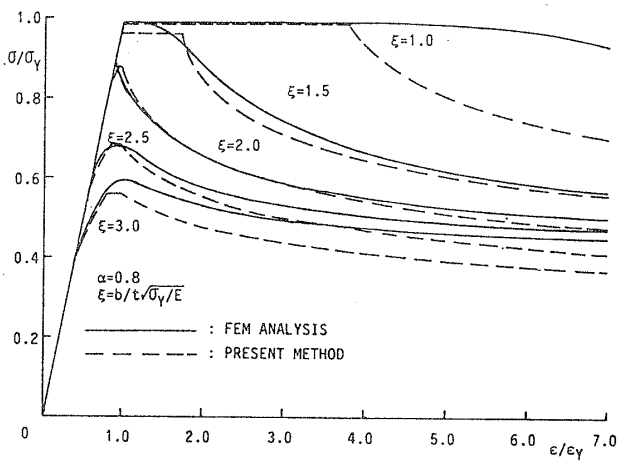

(b) Average stress-strain relationships

Fig. 5 Comparison between calculated results by the present method and FEM (Plate)

$\alpha > 1.0$

$$m_{45} + (\alpha - 1)m_0/2 = \overline{\sigma}^2 \overline{A} \tag{17}$$

Deflection by Eq.(16) is plotted by a dashed line in Fig.5 (a), which shows good agreement with those by FEM analysis.

The average stress-strain relastionships derived by the proposed method are plotted in Fig. 5 (b) comparing with those by FEM analysis. Equation (16) was used to evaluate deflection in the post-ultimate strength range. Good correlations are observed between both results.

2.3 Average Stress-Strain Relationship of Stiffeners with Plating

2.3.1 Assumed deflection mode

A stiffener is assumed to be initiallly deflected along its span in the following mode:

$$w_0 = \delta_0 \sin \frac{\pi x}{a} \tag{18}$$

The total deflection under compressive axial load is expressed as the sum of the elastic and the plastic components.[18]

$$w = w^e + w^p \tag{19}$$

The elastic component is assumed to be in the same mode with initial deflection as follows.

$$w^e = \delta_m \sin \frac{\pi x}{a} \tag{20}$$

According to Ref.19), the coefficient of elastic component is evaluated as:

$$\delta_m = \delta_0/(1 - P/P_{cr}) \tag{21}$$

where P and P_{cr} are the applied compressive load and the elastic buckling load, respectively.

On the other hand, the plastic component is assumed in the following forms:[18]

$0 \leq x < (a - a^p)/2$

$$w^p = 2cx/a \tag{22}$$

$(a - a^p)/2 \leq x \leq a/2$

$$w^p = c\left[-\frac{2x^2}{aa^p} + \frac{2x}{a^p} + 1 - \frac{1}{2}\left(\frac{a}{a^p} + \frac{a^p}{a}\right)\right] \tag{23}$$

From the assumed deflection modes, the curvature K and its elastic and plastic components at the mid-span point are derived as follows:

$$K = K^e + K^p \tag{24}$$

$$K^e = (\pi/a)^2(\delta_m - \delta_0) \tag{25}$$

$$K^p = 4c/aa^p \tag{26}$$

Deflection and curvature components in a single span range are shown in Fig.6.

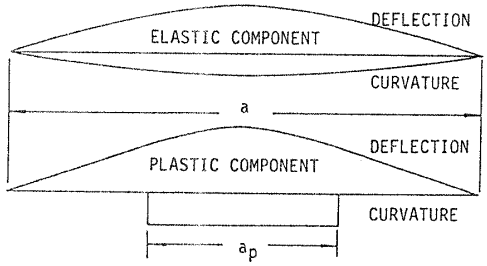

Fig. 6 Elastic and plastic components of deflection and curvature

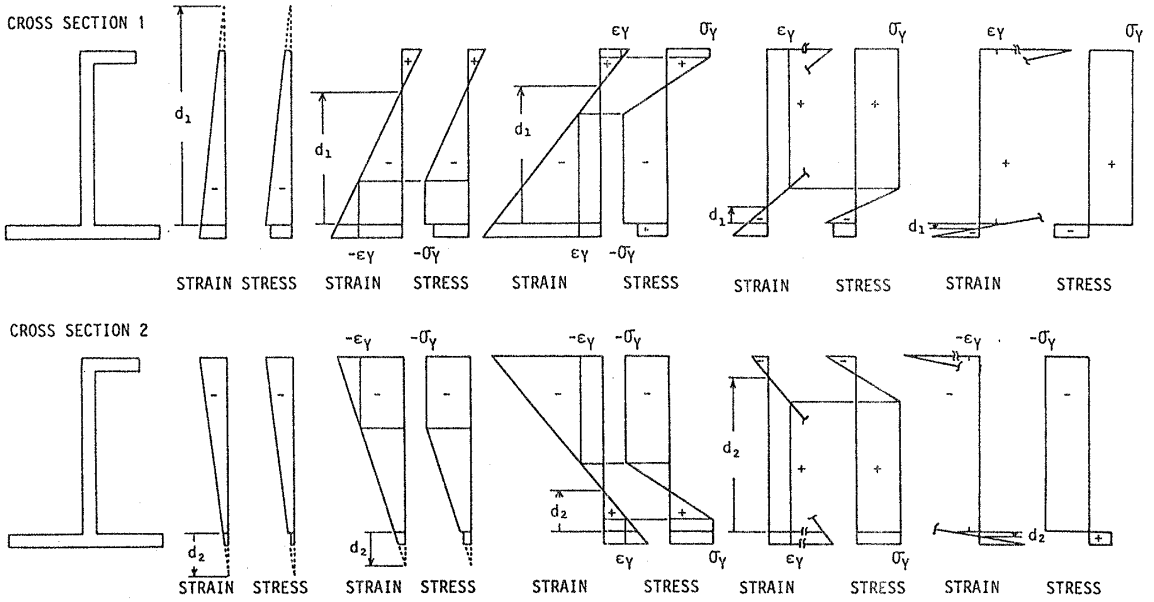

Fig. 7 Possible distributions of strains and stresses at cross-sections, 1 and 2

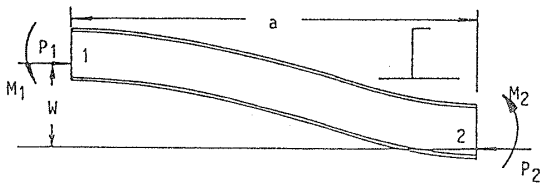

Fig. 8 Forces and moments acting on both ends of stiffener element

2.3.2 Axial force and bending moment at cross-section

The strain and stress distributions at cross-sections *1* and *2* take one of the patterns indicated in Fig.7. In the plate part, the stress-strain relationship derived by the method in 2.2 is used. If unloading is detected in the plate, the stress-strain relationship is assumed to follow the unloading path. Axial forces and bending moments at each cross-section are evaluated by integrating stresses in Fig.7.

2.3.3 Equilibrium conditions

Neglecting the reaction forces at supporting points, the following equilibrium conditions of forces and moments have to be satisfied.

$$P_1 = P_2 \tag{27}$$

$$M_2 + M_1 - W(P_1 + P_2)/2 \tag{28}$$

where P_1, P_2, M_1, M_2 and W are indicated in Fig.8.

Here, if the average stress-strain relationships derived by the method in 2.2 are used for the plating, the effective flexural rigidities at cross-sections *1*and *2* differ each other, since the strains in plating are different at these cross-sections. Consequently, the point of zero bending moment moves along the span from the original supporting point as the axial compressive load increases. Denoting the distances between zero bending moment point and cross-sections *1* and *2* as a_1 and a_2, respectively, the elastic buckling loads for each span are expressed as:

$$P_{cr1} = \pi^2 EI_1/a_1^2, \quad P_{cr2} = \pi^2 EI_2/a_2^2 \tag{29}$$

where EI_1 and EI_2 are the flexural rigidities at cross-sections *1* and *2*, respectively. In deriving Eq.(29), it is assumed that flexural rigidities are the same and equal to those at cross-sections *1* and *2* along the corresponding spans. The lengths of spans a_1 and a_2 are evaluated from the conditions:

$$a_1 + a_2 = 2a \tag{30}$$

$$P_{cr1} = P_{cr2} \tag{31}$$

and are given as:

$$a_1 = 2a/(1+\beta), \quad a_2 = 2a\beta/(1+\beta) \tag{32}$$

where $\beta = \sqrt{EI_2/EI_1}$.

The deflection along each span and the curvatures at cross-sections *1* and *2* are evaluated according to Eqs.(18) through (23) substituting a_1 and/or a_2 into a. When both spans are elastic, the ratio of curvatures at cross-sections *1* and *2* is expressed as follows:

$$K_2/K_1 = 1/\beta \tag{33}$$

2.3.4 Relationship between average stress and average strain

After the equilibrium conditions are satisfied, the axial compressive strain is evaluated by the following equation.

$$\varepsilon = \varepsilon^0 + \frac{1}{2a}\sum_{i=1}^{2}\int_0^{a_i}\left[\varepsilon_i^k + \frac{1}{2}\left(\frac{dw_i}{dx}\right)^2\right]dx \tag{34}$$

where

$$\varepsilon^0 = P/EF$$
$$\varepsilon_i^k = K_i(d_i - e) - \varepsilon^0$$

F, e and d_i represent the sectional area, the location of original neutral axis and the current location of zero stress point. The subscript i indicates the corresponding span or cross-section.

When the element is subjected to tensile axial force, the average stress-strain relationship is assumed to follow that of the elastic-perfectly plastic material. The influence of welding residual stresses in plating is con-

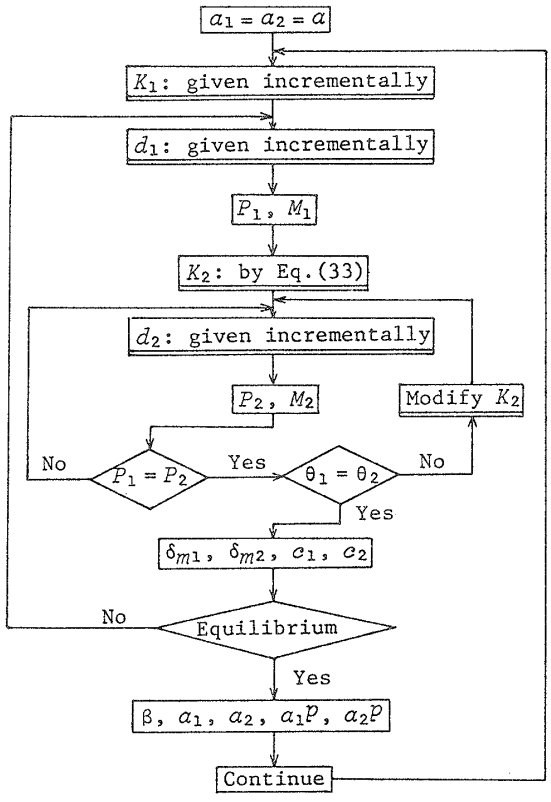

Fig. 9 Flow chart to derive average stress-strain relationship of stiffener element

sidered by reducing rigidity of plating according to Eq.(15).

2.3.5 Procedure to derive average stress- strain relationship

The average stress-average strain relationship is produced according to the flow chart in Fig.9. To evaluate the lengths of yielded zone, a_1^p and a_2^p, the same method is applied as that in Ref.18).

2.3.6 Accuracy of stress-strain relationship by the proposed method

A series of elastoplastic large deflection analysis was performed to examine the accuracy of average stress-strain relationship derived by the proposed method. The shaded part in Fig.10 was analysed with the dimensions indicated in the figure. The plate part was divided into 10 × 30 elements. The calculated average stress-strain curves are plotted in Fig.11 together with those by the proposed method. Although some differences are observed in both results near the ultimate strength, it may be said that the predicted average stress-strain relationship is accurate enough.

2.4 Progressive Collapse Analysis of Cross-Section Subjected to Bi-axial Bending

According to Smith,[11] the equilibrium equation of the cross-section of a girder subjected to bi-axial bending is expressed in the following form.

$$\begin{Bmatrix} \Delta M_H \\ \Delta M_V \end{Bmatrix} = \begin{bmatrix} D_{HH} & D_{HV} \\ D_{VH} & D_{VV} \end{bmatrix} \begin{Bmatrix} \Delta \Phi_H \\ \Delta \Phi_V \end{Bmatrix} \quad (35)$$

where

ΔM_H: increment of horizontal bending moment;
ΔM_V: increment of vertical bending moment;
$\Delta \Phi_H$: increment of horizontal curvature;
$\Delta \Phi_V$: increment of vertical curvature.

D_{HH}, D_{HV}, D_{VH} and D_{VV} are the tangential flexural rigidities of the cross-section, and are calculated as:

$$D_{HH} = \Sigma D_i F_i (y_i - y_g)^2 \quad (36)$$

$$D_{VV} = \Sigma D_i F_i (z_i - z_g)^2 \quad (37)$$

$$D_{HV} = D_{VH} = \Sigma D_i F_i (y_i - y_g)(z_i - z_g) \quad (38)$$

where y_i and z_i are horizontal and vertical coordinates and F_i is the sectional area of the ith element. D_i is the slope of the average stress-strain curve of the ith element at the specified strain. When unloading occurs, the slope of an unloading path is used. y_g and z_g represent the horizontal and vertical coordinates of instantaneous neutral axes for horizontal and vertical bending, respectively. They are calculated as:

$$y_g = (\Sigma F_i y_i D_i)/(\Sigma F_i D_i) \quad (39)$$

$$z_g = (\Sigma F_i z_i D_i)/(\Sigma F_i D_i) \quad (40)$$

At each incremental step, the slope of average stress-strain curve of individual elements at each specified strain is firstly evaluated. Then, the locations of the instantaneous neutral axes are calculated by Eqs.(39) and (40), and the tangential rigidity of the cross-section by Eqs.(36), (37) and (38). After this, for the prescribed increments of curvature, the bending moment increments are evaluated by Eq.(35). The stress increments in the elements are calculated according to the stress-strain curves of individual elements. Then, all the increments are summed to the previous values to provide cumulative values. The influences of both buckling and yielding are automatically accounted using the average stress-strain curves derived by the proposed method.

The computer program "HULLST" was developed to perform such analysis.

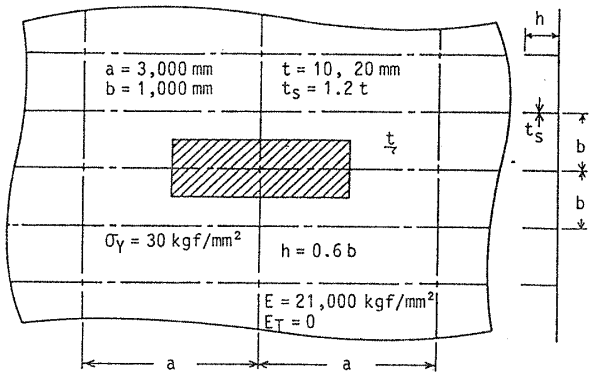

Fig. 10 Stiffened plate for elastoplastic large deflection analysis

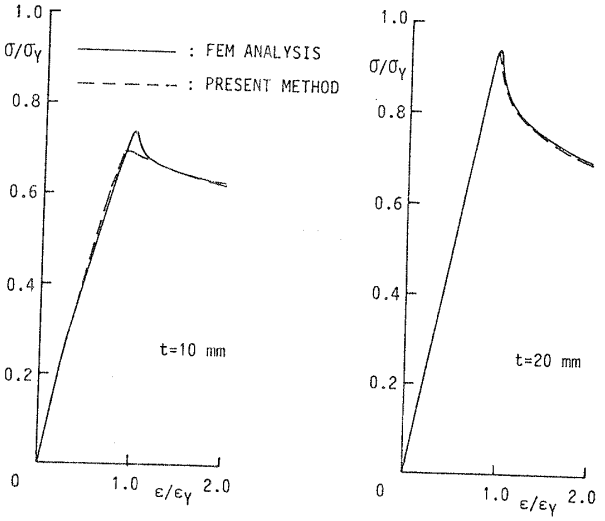

(a) Thin stiffened plate (b) Thick stiffened plate

Fig. 11 Comparison between calculated results by the present method and FEM (Stiffened plate)

3. Numerical Calculations and Discussions

3.1 Calculation on Test Girders

To examine the rationality of the proposed method, a series of progressive collapse analysis was performed on exsisting box girder models[3,20,21] subjected to longitudinal bending. The results of analyses are presented in Ref.22). Here, an alternative analysis[23] was performed on 1/3-scale model of Leander class frigate tested by Dow[24] under four point bending.

Figure 12 shows the cross-section of the test model, of which total dimensions are $L \times B \times D = 18m \times 4.1m \times 2.8m$. The dimensions of main structural components are indicated in the figure together with material properties and initial imperfections due to welding.

In the analysis, two stiffener elements at the deck-side corner and the top plates of deep girders representing the internal deck structures are considered as hard corner elements which do not undergo buckling. Dow[24] also performed the progressive collapse analysis applying the original Smith's method. The results of analyses are shown in Figs.13 (a) and (b).

The solid lines in Fig.13 (a) represent the average stress-strain curves in compression range derived by the present method, and the chain lines by the FEM analysis by Dow for three typical elements, *1*, *2* and *3*, indicated in Fig.12. Significant difference is observed in the elastic rigidities of elements *2* and *3* derived by both method. Concerning the results obtained by the present method, the following comments can be given.

As indicated in Fig.12, plating is accompanied by high residual stresses and large initial deflection. The buckling stresses by elastic calculation considering the influences of these residual stresses are 536.1, 48.0 and -30.1 N/mm^2 for elements *1*, *2* and *3*, respectively. The physical meaning of negative buckling strength is that the plate has been buckled due to compressive residual stresses without any external load. When such buckled plate is subjected to inplane compression, its inplane rigidity is equal to that of a flat plate above buckling strength from the beginning of loading. Such behaviour is automatically simulated by the present method. For the plating analysed here, the inplane rigidity above buckling strength is $E/2$. This

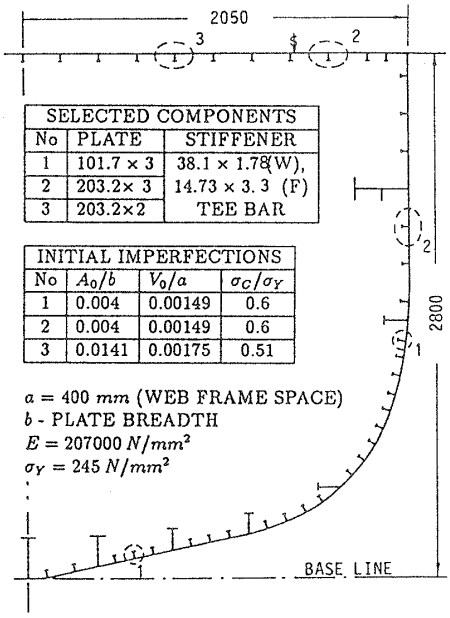

Fig. 12 Midship section of 1/3-scale frigate model

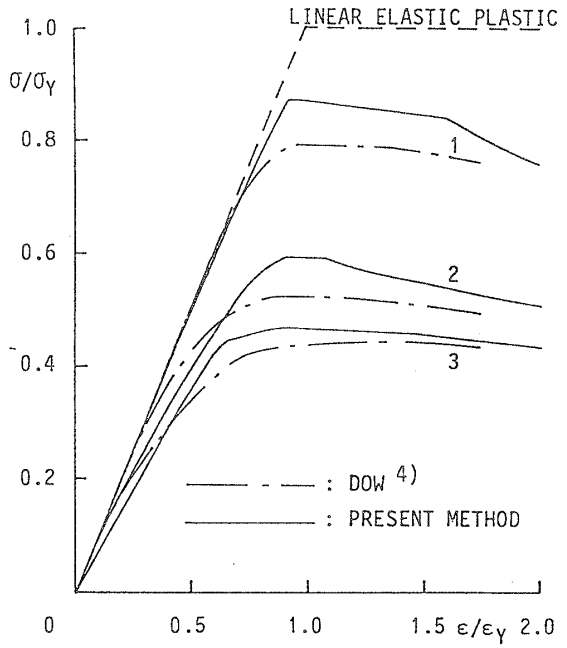

(a) Element stress-strain relationships in compression

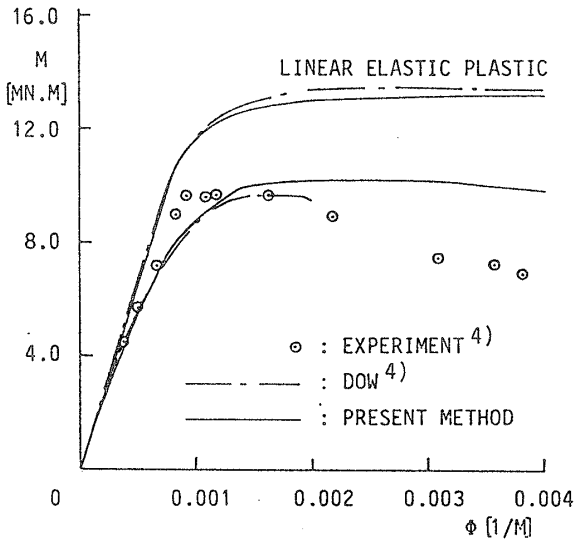

(b) Moment-curvature relationships under sagging condition

Fig. 13 Results of analysis for frigate model

may be the main reason of the reduced rigidity of element *3* from the beginning of loading. The rigidity of element *2* is reduced from the early stage of loading also due to high compressive residual stresses.

The calculated and measured moment-curvature relationships are compared in Fig.13 (b). The solid and chain lines represent the calculated results by the present method and Dow[24], respectively. The measured results are indicated by ⊙. Concerning the ultimate strength, the experimental and two numerical results are in a very good agreement each other.

In the experiment, fairly large overall vertical deflections were observed at the main strength deck due to overall grillage buckling, but this buckling did not show a significant influence on the hull girder moment-curvature response according to Dow[24]. He also described in his paper that "Approaching the ultimate load, local stiffener and plating deformations developed on the deck, superimposed on the overall deck deformation, precipitating deck collapse. The side shell clearly showed interframe buckling of the longitudinal stiffeners with associated plate buckling". The predicted collapse mode is also interframe flexural buckling of the deck stiffener elements.

Some differences appear between the measured and calculated flexural rigidity of the cross-section especially at a higher load level. According to Dow[24], a possible source of error was in the computation of the experimental curvature of the hull calculated with the vertical displacements, which, when significant nonlinearities occur, would underestimate the local curvature of the hull in the region of collapse. The assumption that the plane-sections remain plane may also lead to the differences between measured and calculated moment-curvature relationship after the ultimate strength when large deformations are produced.

3.2 Calculation on Existing Bulk Carrier

Progressive collapse analysis was performed on the hull girder of an existing bulk carrier of 60,000 *DWT*. The principal dimensions are shown in Fig.14. *HT*36 steel was used at the deck plating and the upper parts of the sloped bulkhead of top side tank and the side plating, and *HT*32 steel in the remaining part. In the analysis, the welding residual stresses of $2b_t/b = 0.1$ was assumed in the plating between stiffeners, and the initial deflections of $A_0/t = 0.01$ and $\delta_0/a = 0.002$ in plating and stiffeners, respectively. At the corner part of the cross-section, hard corner elements were introduced. For some typical elements, the calculated average stress-strain curves are plotted in Fig.15 (a). Both hogging and sagging moments were applied, and the calculated moment-curvature curves are shown in Fig.15 (b).

In Fig.15 (b), the dashed line represents the result when all elements are assumed to follow the stress-strain relationship of an elastic-perfectly plastic material. All the elements are free from initial imperfections and do not undergo buckling. In this case, the same results are obtained under hogging and sagging conditions, and the ultimate strength is equal to the fully plastic bending moment of the cross-section. On the other hand, solid and chain lines represent the moment-curvature curves when elements behave following the average stress-strain curves such as those shown in Fig.15 (a). It is known from Fig.15 (b) that a fully plastic bending moment can not be sustained at the cross-section bacause of local buckling collapses.

The slope of a moment-curvature curve represents the tangential flexural rigidity of the cross-section. It is observed in Fig.15 (b) that flexural rigidity is reduced from the beginning of loading when initial imperfections are introduced. This is partly because of initial deflections, but mainly due to welding residual stresses in tension. When a plate with welding residual stresses is subjected to tensile load, the portions where tensile residual stresses exist can not carry tensile load, since these portions are already yielded in tension. This results in a reduced inplane rigidity of the elements in tension range which is almost a half cross-section.

In Fig.15 (b), numerals and alphabets on the curves indicate the loading steps, at which stress distribution and collapse state are illustrated in Figs.16 (a) and (b).

Under the hogging condition, at point *a*, the initial local collapse takes place at the deck plating by yielding in tension as indicated in Fig.16 (a). With further increase in the applied curvature, yielding spreads all over the deck and at the upper parts of side shell and sloped bulkhead of top side tank. At the same time, bottom plate and inner bottom plate buckle, and the ultimate strength is attained at point *b*. At this point,

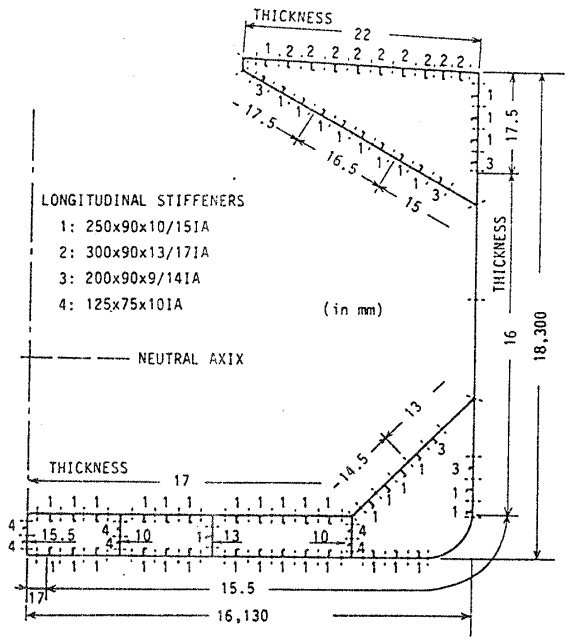

Fig. 14 Midship section of bulk carrier (60,000 DWT)

the whole top side tank is yielded in tension. After the ultimate strength, buckled part spreads over the sloped bulkhead of hopper side tank and the lower part of side shell, but unloading takes place at some parts of the tensile region of bending, as is known observing the yielded parts and stress distributions at points *b*, *c* and *d* in Fig.16 (a). This is because the load carried at buckled double bottom and hopper side tank decreases, and the neutral axis moves upward.

Under the sagging condition, at point *1*, the initial collapse takes place at the uppermost stiffener of the sloped bulkhead of top side tank by buckling as indicated in Fig.16 (b). With further increase in the applied curvature, buckled part spreads and, at point *2*, the ultimate strength is attained. The reserve strength after the initial collapse is very small compared to the case of the hogging condition. In both cases, the collapse starts to take place at the upper part of a cross-section. The collapse under the hogging condition occurs by yielding and no reduction exists in the load

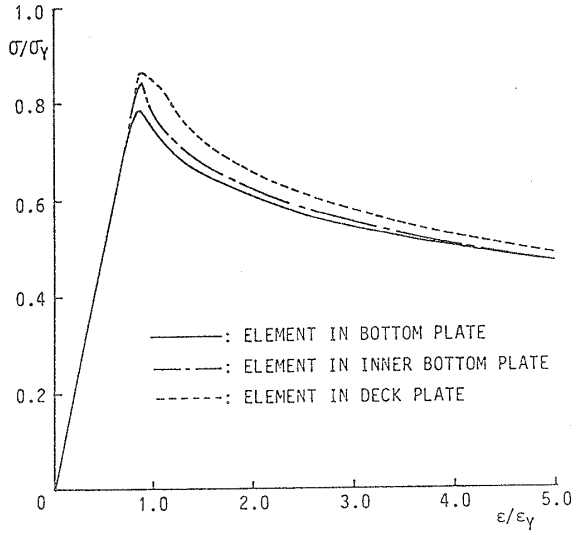

(a) Element stress-strain relationships in compression

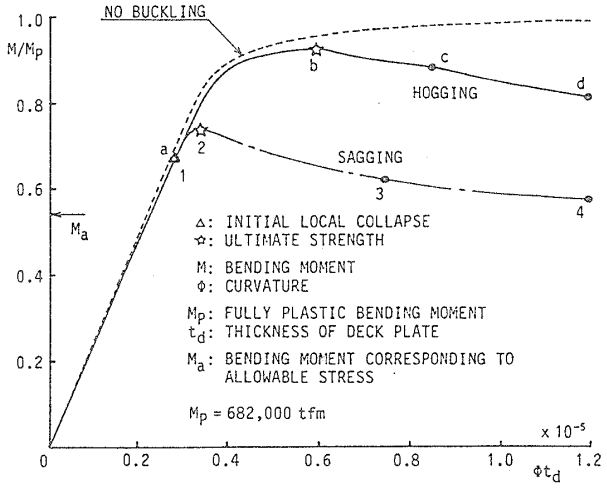

(b) Moment-curvature relationships

Fig. 15 Results of analysis for bulk carrier

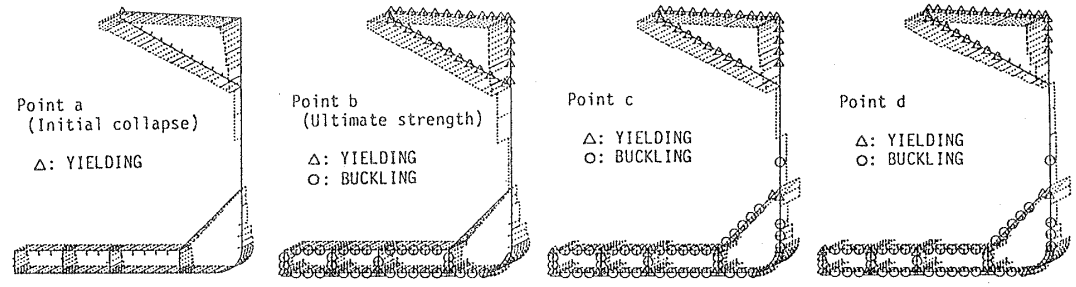

(a) Hogging condition

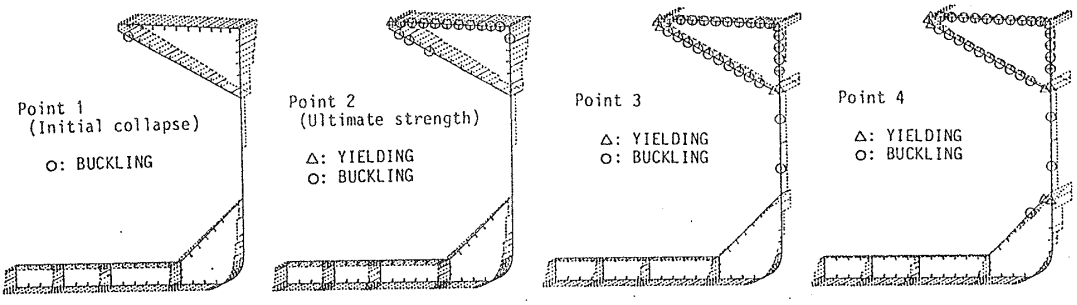

(b) Sagging condition

Fig. 16 Stress distributions and failure modes

carrying capacity of collapsed members after their ultimate strength, whereas collapse under the sagging condition occurs by buckling and singinficant reduction exists in load carrying capacity after ultimate strength. This leads to the significant difference in reserve strength after initial collapse under the sagging and the hogging conditions. With further increase in applied curvature, the buckled part spreads downward. This results in the downward movement of neutral axis, and yielding in tension did not occur within the applied curvature shown in Fig.16 (b).

According to the Rules by Classification Societies, the allowable stress is specified. The allowable bending moment corresponding to the allowable stress is calculated according to the Rule by Lloy'd Register of Shipping[25], and is indicated in Fig.15 (b). It is known that this ship has enough strength as far as the ultimate longitudinal strength is concerned.

4. Conclusions

A simple method was proposed to simulate the progressive collapse behaviour of hull girder cross-section under longitudinal bending. This method takes into account of the progressive loss in rigidity due to the occurrence of local buckling and yielding. The fundamental idea of this method follows to that proposed by Smith.[9-13] In this method, a cross-section is divided into small elements composed of plates and stiffeners. In this paper, a simple analytical method was proposed to derive the average stress-strain relationship of individual elements. The proposed method is as follows:

(1) A double span model is considered that takes adjacent two midspan points between transverse frames as both ends of the element. The cross-section is composed of a stiffener and half breadths of plating between stiffeners on each side of the stiffener.

(2) The average stress-strain relationship of the attached plate is derived by combining the results of elastic large deflection analysis and plastic mechanism analysis both in analytical forms.

(3) The deflection of a stiffener is expressed as the sum of an elastic component in a sinusoidal mode and a plastic component that gives a constant curvature in the midspan part.

(4) Assuming linear distributions of strains, the elastoplastic stress distributions at both ends of the element are determined which satisfy equilibrium conditions of forces and moments. At the plate parts, the average stress-strain curves derived in (2) are used.

(5) Axial strain is evaluated with the axial force and deflection.

Example calculation was carried out on a 1/3-scale frigate model tested by Dow[24], and the rationality of the proposed method was confirmed. Then, progressive collapse analysis was performed on the cross-section of an existing bulk carrier both under hogging and sagging conditions. It was shown that the cross-section can not carry the fully plastic bending moment due to the occurrence of local buckling in the compression side of bending. More decrease was observed in ultimate strength under the sagging condition than under the hogging condition.

In the present paper, the assumed deflection mode for a stiffener was only that of an Eulerian buckling mode. In Ref.23), the present method was improved by introducing deflection component of torsional buckling, and considering flexural-torsional buckling of a stiffener. As for a loading condition when element stress-strain curves are calculated, only the axial load is considered. For the actual case, however, the influences of lateral pressure acting at the bottom plate and inplane shear force produced in side shell have to be included. These remain as future works.

References

1) Chen, Y. K., Kutt, L. M., Piaszczyk, C. M. and Bieniek, M. P.: "Ultimate Strength of Ship Structures", Trans. SNAME, Vol.91 (1983), pp.149-168.
2) Kutt, L. M., Piaszczyk, C. M. and Chen, Y. K.: "Evaluation of the Longitudinal Ultimate Strength of Various Ship Hull Configurations", Trans. SNAME, Vol,93 (1985), pp.33-55.
3) Nishihara, S.: "Analysis of Ultimate Strength of Stiffened Rectangular Plate (4th Report) - On the Ultimate Bending Moment of Ship Hull Girder -", J. Soc. Naval Arch. of Japan, Vol.154 (1983), pp.367-376 (in Japanese).
4) Endo, H., Tanaka, Y., Aoki, G., Inoue, H. and Yamamoto, Y.: "Longitudinal Strength of the Fore Body of Ships Suffering from Slamming", J. Soc. Naval Arch. of Japan, Vol.163 (1988), pp.322-333 (in Japanese).
5) Ueda, Y., Rashed, S. M. H. and Paik, J. K.: "Plate and Stiffened Plate Units of The Idealized Structural Unit Method (1st Report) - Under Inplane Loading -", J. Soc. Naval Arch. of Japan, Vol.156 (1984), pp.366-377 (in Japanese).
6) Ueda, Y. and Rashed, S.M.H.: "The Idealized Structural Unit Method and Its Application to Deep Girder Structures", Computer and Structures, Vol.18, No.2 (1984), pp.227-293.
7) Paik, J.K. and Lee, D.H.: "Ultimate Longitudinal Strength-Based Safety and Reliability Assessment of Ship's Hull Girder", J. Soc. Naval Arch. of Japan, Vol.168 (1990), pp.397-409.
8) Paik, J. K.: "Ultimate Longitudinal Strength-Based Safety and Reliability Assessment of Ship's Hull Girder (2nd Report) - Stiffened Hull Structure -", J. Soc. Naval Arch. of Japan, Vol.169 (1991), pp.403-414.
9) Smith, C.S.: "Influence of Local Compressive Failure on Ultimate Longitudinal Strength of a Ship's Hull", Proc. PRADS, A-10, Tokyo, Japan (1977), pp.72-79.
10) Dow, R. S., Hugill, R. C., Clarke, J.D. and Smith, C.S.: "Evaluation of Ultimate Ship Hull Strength", Proc. Symp. on Extreme Loads Response, Arlington, USA (1981), pp.131-148.

11) Smith, C. S.: "Structural Redundancy and Damage Tolerance in Relation to Ultimate Ship-Hull Strength", Proc. Int. Symp. on The Role of Design Inspection and Redundancy in Marine Structural Reliability", Williamsburg, USA (1983).
12) Faulkner, J.A., Clarke, J.D., Smith, C.S. and Faulkner, D.: "The Loss of HMS COBRA - A Reassessment", Trans. RINA, Vol.127 (1984), pp.125-151.
13) Creswell, D.J. and Dow, R.S.: "The Application of Nonlinear Analysis to Ship and Submarine Structures", Proc. Int. Conf. on Advances in Marine Structures, ARE, Dunfermline, Scotland (1986), pp.174-200.
14) Caldwell, J.B.: "Ultimate Longitudinal Strength" Trans. Rina, Vol.107 (1965), pp.411-430.
15) Ueda, Y. and Yao, T.: "The Influence of Complex Initial Deflection Modes on Behaviour and Ultimate Strength of Rectangular Plates in Compression", J. Constructional Steel Research, Vol.5, No.4 (1985), pp.265-302.
16) Yao, T. and Nikolov, P.I.: "Stiffness of plates after Buckling", Trans. Kansai Soc. Naval Arch., Vol.215 (1991), pp.137-146.
17) Okada, H., Ohshima, K. and Fukumoto, Y.: "Compressive Strength of Long Rectangular Plates under Hydrostatic Pressure", J. Soc. Naval Arch. of Japan, Vol.146 (1979), pp.101-114 (in Japanese).
18) Yao, T., Fujikubo, M., Bai, Y., Nawata, T. and Tamahiro, M.: "Local Buckling of Bracing Members in Semi-submersible Drilling Unit (1st Report)", J. Soc. Naval Arch. of Japan, Vol.169 (1986), pp.359-371 (in Japanese).
19) Timoshenko, S. P. and Gere, J.M.: Theory of Elastic Stability, 2nd Ed., McGrow-Hill, 1961.
20) Reckling, K.A.: "Behaviour of Box Girders under Bending and Shear", Proc. ISSC, Paris (1979), pp.II-2.46-II.2.49.
21) Dowling, P.J., Moolani, F.M. and Friez, P.A.: "The Effect of Shear Lag on the Ultmate Strength of Box Girder", Proc. Int. Cong. on Steel Plated Structures, London (1976), pp.108-147.
22) Yao, T. and Nikolov, P.I.: "Progressive Collapse Analysis of a Ship's Hull under Longitudinal Bending", J. Soc. Naval Arch. of Japan, Vol.170 (1991), pp.449-461.
23) Yao, T. and Nikolov, P.I.: "Progressive Collapse Analysis of a Ship's Hull under Longitudinal Bending (2nd Report)", J. Soc. Naval Arch. of Japan, Vol.172 (1992), pp.437-446.
24) Dow, R. S.: "Testing and Analysis of a 1/3-Scale Welded Steel Frigate Model", Proc. Int. Conf. on Advances in Marine Structures, ARE, Dunfermline, Scotland (1991), pp.749-773.
25) Lloyd's Resister of Shipping: Rules and Regulations for the Classification of Ships, Part 3, Chap.4, Ship Structures, London (1982),pp.1-6.